JOURNAL OF AGRICULTURAL AND FOOD CHEMISTRY

Metalloporphyrins as Biomimetic Models for Cytochrome P-450 in the Oxidation of Atrazine

MARIA C. A. F. GOTARDO, LUIZ A. B. DE MORAES, AND MARILDA D. ASSIS*

Departamento de Química, Faculdade de Filosofia Ciências e Letras de Ribeirão Preto, Universidade de São Paulo, Av. Bandeirantes 3900, 14040-901 Ribeirão Preto, SP, Brazil

The aim of this work was to evaluate whether metalloporphyrin models could mimic the action of cytochrome P-450 in the oxidation of atrazine, a herbicide. The commercially available second-generation metalloporphyrins 5,10,15,20-tetrakis(2,6-dichlorophenyl)porphyrin metal(III) chloride [M(TDCPP)Cl] and 5,10,15,20-tetrakis(pentafluorophenyl)porphyrin metal(III) chloride [M(TFPP)Cl] (metal = Fe or Mn) and the oxidants iodosylbenzene and metachloroperbenzoic acid were employed in this study. Results showed that the metalloporphyrins used here can oxidize atrazine. Yields as high as 32% were obtained for the Mn(TFPP)Cl/PhIO system, which shows that these catalysts can mimic both the in vivo and the in vitro action of cytochrome P-450, with formation of the metabolites DEA and DIA. The formation of five other unknown products was also detected, but only one of them could be identified, since the other four were present in very low concentrations. The compound COA, identified by mass spectrometry, was the main product in most of the oxidation reactions.

KEYWORDS: P450; herbicide metabolism; metalloporphyrin; atrazine

INTRODUCTION

The cytochrome P-450 enzymes (P450) are one of the most important systems responsible for pesticide detoxification in plants (*1*, *2*). Increased P450 activity is related to the development of a resistance mechanism by weeds through which toxic compounds are metabolized and thus inactivated. Therefore, understanding the way these enzymes act, as well as gaining knowledge about the potential development of plant resistance to new pesticides on the part of weeds, has become of great importance for control of herbicide tolerance in plantations and weeds, as well as for optimization of novel active compounds to be used in agriculture (*1*, *3*).

The majority of the studies showing the role of P450 in the transformation of herbicides in weeds have been carried out in vivo. This is because isolating enough amounts of microsomal fractions from these plants is extremely difficult. As for higher plants, the participation of P450 in herbicide detoxification can be investigated by using plant microsome in vitro assays (*1*).

As the isolation of P450 genes from plants is extremely difficult, the first reactions employing this hemoprotein's genes were carried out with bacterial and mammalian P450. Only in recent years have genes of P450 enzymes been isolated from plants, and the first reactions confirmed that these enzymes take an active part in herbicide detoxification (*1*).

The use of chemical model systems mimicking P450 might therefore be a very useful tool for overcoming the difficulty in working with enzymes in vivo and in vitro, and these models may help scientists understand detoxification mechanisms, thus enabling the development of novel pest inhibitors (*4*).

In this context, synthetic metalloporphyrins have been used as biomimetic models for more than 20 years, especially in drug metabolism studies (*5*, *6*). These complexes have provided a better understanding of the metabolism of active compounds in vivo by helping to identify which functional groups in the new drugs are sensitive to metabolism. This information has enabled the large-scale production of metabolites (on the scale of milligrams) for pharmacological studies and toxicological tests.

Despite the good results obtained with the use of synthetic metalloporphyrins in drug oxidation, few studies have been devoted to the application of these models in pesticide transformation. Keserü and co-workers are one of the few groups working in this field, and they have shown that Fe(TFPP)Cl can mimic the action of insect P450 in the chemical transformation of insecticides belonging to the carbamate class of compounds (*7*).

Fukushima et al. have recently compared the metabolism of the insecticide pyriproxyfen in tomatoes with results obtained by means of a biomimetical study employing metalloporphyrin models (*8*). These authors succeeded in showing that metalloporphyrins are able to mimic the in vivo action of P450.

Atrazine (2-chloro 4-ethylamino-6-isopropylamino-1,3,5-triazine; ATZ) is a pre- and post-emerging selective herbicide for weed control. This compound acts as an effective inhibitor of the Hill reaction in photosynthesis, thus reducing the amount of CO_2 fixed in the plant (*9*−*12*). This compound is extremely important in agriculture, especially because of its tolerance by

* Corresponding author. Telephone: +55 16 36023799. Fax: +55 16 36023848. E-mail: mddassis@usp.br.

10.1021/jf062462n CCC: $33.50
Published on Web 12/08/2006

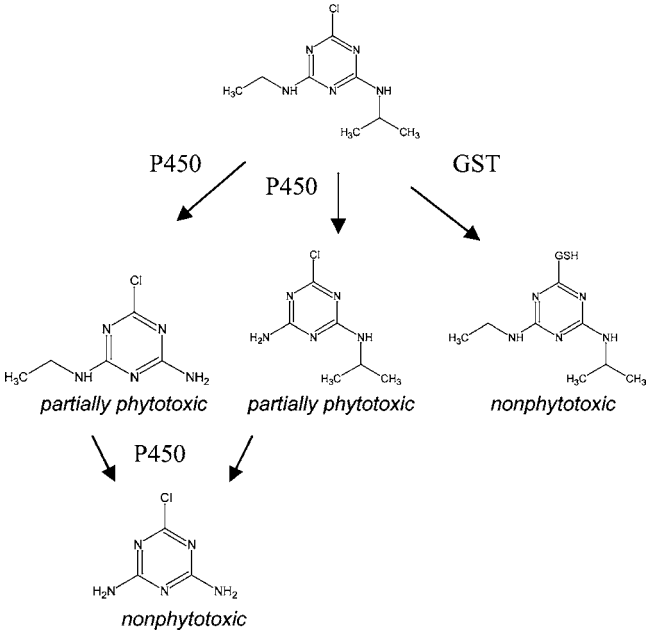

Figure 1. Atrazine metabolism in corn (adapted form ref 11).

maize. In fact, it is one of the most widely employed herbicides in the United States.

In this culture, the main herbicide detoxification routes consist of glutathione conjugation catalyzed by glutathione s-transferase and N-dealkylation, as shown in **Figure 1**. Although P450 is thought to catalyze N-dealkylation, this has not been demonstrated in vivo.

The first N-dealkylation reduces herbicide affinity for the target receptors, thus reducing its toxicity. The second N-dealkylation culminates with herbicide detoxification in the plant (*12*).

In the environment, the main ATZ metabolites are its N-dealkylated products. Nevertheless, this herbicide is highly persistent and mobile, being one of the main underground water contaminants in Europe. Degradation of this compound by microbial catalysis in soil environments is a relatively slow process, with a half-life of 60−100 days (*13*, *14*).

The aim of this work is to evaluate whether metalloporphyrin systems can mimic the action of P450 in the oxidation of atrazine. To this end, we employed the commercially available second-generation metalloporphyrins 5,10,15,20-tetrakis(2,6-dichlorophenyl)porphyrin metal(III) chloride [M(TDCPP)Cl] and 5,10,15,20-tetrakis(pentafluorophenyl)porphyrin metal(III) chloride [M(TFPP)Cl] (metal = Fe or Mn).

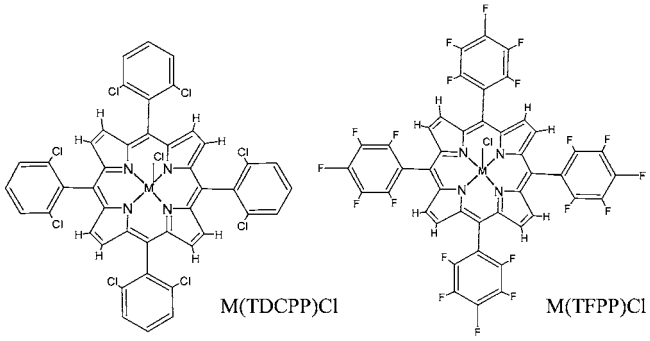

Figure 2. Metallopophyrins used in this study (M = Fe^{III} or Mn^{III}).

2. MATERIALS AND METHODS

All the chemicals used in this work were HPLC-grade or P.A., purchased from Merck, Aldrich, Acros, Fluka, or Mallinckrodt, and used as received. Atrazine (99.2% purity) was provided by Supelco and Syngenta. Deethylatrazine (99.9% purity), deisopropylatrazine (96.1% purity), deethyldeisopropylatrazine (98.3% purity), hydroxyatrazine (96.0% purity), deethylhydroxyatrazine (98.7% purity), and deethyldeisopropylhydroxyatrazine (99.6% purity) were provided by Supelco. **Table 1** lists the structures, common names, chemical names, and abbreviations of atrazine and its metabolites. Metachloroperbenzoic acid (*m*-CPBA) was provided by Acros (70% purity). Iodosylbenzene (PhIO) was prepared by hydrolysis of iodosylbenzene diacetate, following the method of Sharefkin and Saltzman (*15*), and its purity was 93%, as determined by iodometric titration. Imidazole (Im) was provided by Acros (99% purity). The porphyrins Fe(TFPP)Cl, H_2(TDCPP), and H_2(TFPP), were purchased from Mid-Century and used as received. Iron and manganese insertion into the free base porphyrins H_2(TDCPP)Cl and H_2(TFPP)Cl was carried out using the method of Adler et al. (*16*). **Figure 2** shows the structures of the metalloporphyrins used in this study.

2.1. Oxidation Reactions. The standard catalyst/oxidant/substrate molar ratio used in the oxidation of atrazine was 1:60:120. To this end, 2.5×10^{-7} mol of the metalloporphyrin, 1.5×10^{-5} mol of the oxidant, and 3×10^{-5} mol of ATZ in 1500 μL of solvent were employed (MeOH or ACN). Another catalyst/oxidant/substrate molar ratio with excess oxidant was also used, namely 1:240:120. Imidazole was added to some reactions, at a catalyst/ligand molar ratio of 1:10. All reactions were carried out at room temperature under magnetic stirring. At the end of the reaction (24 h) or at regular intervals, an aliquot of the reaction mixture (200 mL) was withdrawn. The porphyrin was removed from this aliquot before analysis by HPLC, by addition of hexane (600 mL) and a mobile phase (400 mL). This mixture was vortex-mixed and centrifuged; the lower phase (mobile phase) containing the oxidation products was then injected into the chromatographic system.

2.2. HPLC Analysis. The analytical HPLC analyses were performed on a SHIMADZU liquid chromatograph equipped with an LC-10AS

Table 1. Chemical Structure of Atrazine and Its Metabolites

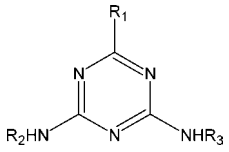

abbreviations	compounds	R1	R2	R3
ATZ	2-chloro-4-(isopropylamino)-6-(ethylamino)-*s*-triazine (atrazine)	–Cl	$-CH_2CH_3$	$-CH(CH_3)_2$
DEA	2-chloro-4-(isopropylamino)-6-amino-*s*-triazine (deethylatrazine)	–Cl	–H	$-CH(CH_3)_2$
DIA	2-chloro-4-(ethylamino)-6-amino-*s*-triazine (deisopropylatrazine)	–Cl	$-CH_2CH_3$	–H
DAA	2-chloro-4,6-diamino-*s*-triazine (deethyldeisopropylatrazine)	–Cl	–H	–H
OHA	2-hydroxy-4-(isopropylamino)-6-(ethylamino)-*s*-triazine (hydroxyatrazine)	–OH	$-CH_2CH_3$	$-CH(CH_3)_2$
OHDEA	2-hydroxy-4-(isopropylamino)-6-amino-*s*-triazine (deethylhydroxyatrazine)	–OH	–H	$-CH(CH_3)_2$
OHDAA	2-hydroxy-4,6-diamino-*s*-triazine (deethyldeisopropylhydroxyatrazine)	–OH	–H	–H
COA	2-chloro-4-(acetamido)-6-(isopropylamino)-*s*-triazine	–Cl	$-NHCOCH_3$	$-NHCH(CH_3)_2$

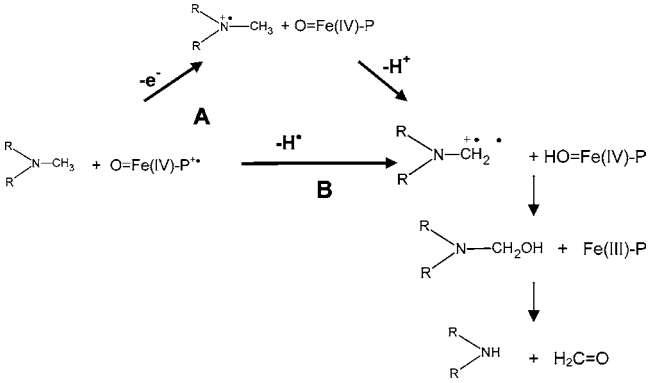

Figure 3. Mechanism of P450-catalyzed N-dealkylations.

solvent pump, an SPD-M 10A VP spectrophotometric detector (λ = 220 nm) coupled to a CTO-10A VP column oven, and an SCL-10A VP system controller. Separation of the herbicide and the oxidation products was carried out in a Lichrospher 100RP-18 column, with a particle size of 5 μm (125 mm × 4 mm), supplied by Merck. The analytical column was protected by a LiChrospher guard column (4 mm × 4 mm). Elution was carried out with a gradient ranging from phosphate buffer (pH 7)/methanol 90:10 (v/v) to phosphate buffer (pH 7)/methanol 50:50 (v/v), at a flow rate of 1.0 mL min^{-1}. The run time was 40 min. The mobile phase was purged with helium.

2.3. Mass Spectrometry Analysis. Products generated from the metalloporphyrin-catalyzed atrazine oxidation were collected separately by means of an HPLC collector, stored, and analyzed by mass spectrometry (MS). Elution was carried out with a gradient of ACN/MeOH/acetic acid 0.1% ranging from 8:12:80 v/v to 20:30:50 v/v, at a flow rate of 1.0 mL min^{-1}.

Mass spectra were obtained on a Quattro LC mass spectrometer (Micromass) equipped with an ionization electrospray source in the positive mode (ESI+).

2.4. Nash Test. The Nash reagent (5 mL; 37.5 g of ammonium acetate, 0.75 mL of acetic acid, and 0.5 mL of pentane-1,4-dione in 250 mL of distilled water) (*17*) was added to an aliquot of the reaction mixture (500 μL) in a 10-mL volumetric flask, and the volume was completed with distilled water. This solution was incubated at 40 °C for 40 min, and the solution absorbance was recorded at 412 nm.

2.5. Catalytic Intermediate Studies through UV−Vis Spectra. UV−vis spectra were obtained on a Hewlett-Packard 8452, diode array spectrometer. A quantity of 500 μL of PhIO solution (0.02 mol L^{-1}) was added to a quartz cell (10-mm de path length) containing 1000 μL of Fe(TFPP) and ATZ solution in MeOH or ACN (2×10^{-6} and 1.8×10^{-5} mol L^{-1}, respectively). Consecutive spectra were recorded.

2.6. Catalytic Intermediate Studies through EPR Spectra. The EPR spectra were recorded on a Varian E-4 spectrometer operating at the X band frequency (9 GHz) with a gain of 10^3, 200 mW microwave power, and 10 G amplitude modulation at 4 K. Quantities of 100 μL of PhIO solution (0.02 mol L^{-1}) and 100 μL of ATZ (0.04 mol L^{-1}) were added to an EPR tube containing 100 μL of Fe(TFPP)Cl solution in ACN (3.3×10^{-4} mol L^{-1}). The mixture was stirred manually. Consecutive spectra were recorded.

3. RESULTS AND DISCUSSION

P450-catalyzed ATZ metabolism occurs via N-dealkylation of the ethyl and propyl side chains of the secondary amines in various biological systems (*1*, *2*). According to reports in the literature, P450-catalyzed N-dealkylations occur via initial iron(III)porphyrin oxidation, which gives the high-valent catalytic species oxoferrylporphyrin π-cation radical, Fe(IV)OP$^{\bullet+}$. Thereafter, there are two proposed mechanisms for the reaction, as shown in **Figure 3**.

The first mechanism (A) is known as the electron-transfer mechanism, where there is a one-electron transfer from the substrate to the catalytically active species Fe^{IV}OP$^{\bullet+}$, rendering the ferryl species Fe^{IV}OP. This is followed by hydrogen atom abstraction from the substrate by the latter species, with formation of Fe^{IV}OHP and the substrate radical. Further OH group transfer from Fe^{IV}OHP to the substrate radical results in hydroxylation of the carbon adjacent to the nitrogen atom, leading to an unstable carbinolamine that decomposes into an amine and a carbonyl derivative.

In the second mechanism (B), known as hydrogen abstraction, there is no electron transfer. The catalytically active species Fe^{IV}OP$^{\bullet+}$ directly abstracts a hydrogen atom from the substrate, and the remaining steps are similar to those involved in mechanism (A) (*18*).

In general, the occurrence of either mechanism A or B depends on the substituents present on the nitrogen atom of the substrate (*18*). The mechanism of P450-catalyzed atrazine N-dealkylation is unknown, which makes studies employing P450 chemical models an important tool for its investigation.

In this work, therefore, atrazine oxidation reactions were carried out in the presence of Fe(TFPP)Cl, Fe(TDCPP)Cl, Mn(TFPP)Cl, and Mn(TDCPP)Cl (**Figure 2**), which are all commercially available second-generation metalloporphyrins well-established in the literature as good catalysts for hydrocarbon and drug oxidations (*5*). Contrary to first-generation metalloporphyrins, these compounds bear electron-withdrawing substituents (−Cl or −F) in the *meso*-phenyl positions of the porphyrin macrocycle, which confer steric hindrance to the catalyst and avoid its self-oxidative destruction (*5*). These substituents also activate the catalytic species, generally an oxometal porphyrin cation radical [Me(IV)OP$^{\bullet+}$ or Me(V)OP], making this species more electrophilic and reactive toward the substrate.

PhIO, a two-electron oxidant, was initially used as an oxygen donor in the present study because it is considered a standard oxidant in the case of metalloporphyrin systems (*19*). Later, *m*-CPBA, a peracid that is soluble in organic media and is very frequently used in metalloporphyrin-catalyzed reactions, was also used. The latter oxidant may undergo heterolytic cleavage upon its coordination to the metalloporphyrin central metal ion, leading to the formation of the active species oxoferryl or oxomanganyl porphyrin π-cation radical, Me(IV)OP$^{\bullet+}$. Homolytic cleavage of the O−O bond may also occur, leading to the formation of a less reactive intermediate, Me^{IV}P−OH, as well as RO$^{\bullet}$ radicals, thus favoring the occurrence of radicalar mechanisms (*20*, *21*).

ATZ oxidation reactions were carried out in MeOH and ACN, taking the solubility of this herbicide and its metabolites in these solvents into account. Solubility was also a determining factor for the choice of reaction conditions, once the studied substrate was a solid with limited solubility in the volume employed in the reactions (1.5 mL). A catalyst/oxidant/substrate molar ratio of 1:60:120, corresponding to 2.5×10^{-7} mol of catalyst, 1.5×10^{-5} mol of oxidant, and 3.0×10^{-5} mol of substrate (~7 mg ATZ /1.5 mL of solvent), was the standard condition in our studies.

Control reactions were carried out in the absence of metalloporphyrin, under the same conditions as the catalytic runs, and gave no products.

Table 2 shows the total product yield (*R*%) obtained in the ATZ oxidation reactions for each metalloporphyrin/oxidant system, under different conditions. **Figures 4** and **5** show the plots of relative product distribution, in percent, in the case of the reactions carried out in ACN.

From **Table 2**, it can be seen that the metalloporphyrins studied here are poor catalysts for atrazine oxidation in MeOH, leading to product yields of only around 1%. The catalytic

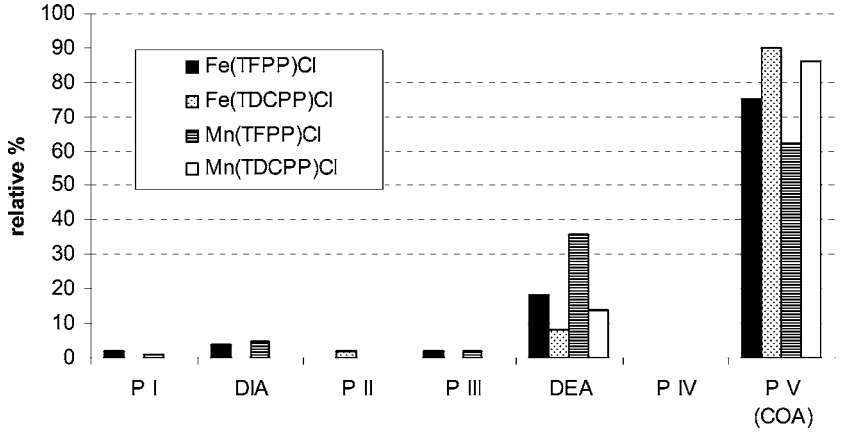

Figure 4. Product distribution (in percentage) obtained in the metalloporphyrin-catalyzed oxidation of ATZ by PhIO in ACN in the standard conditions.

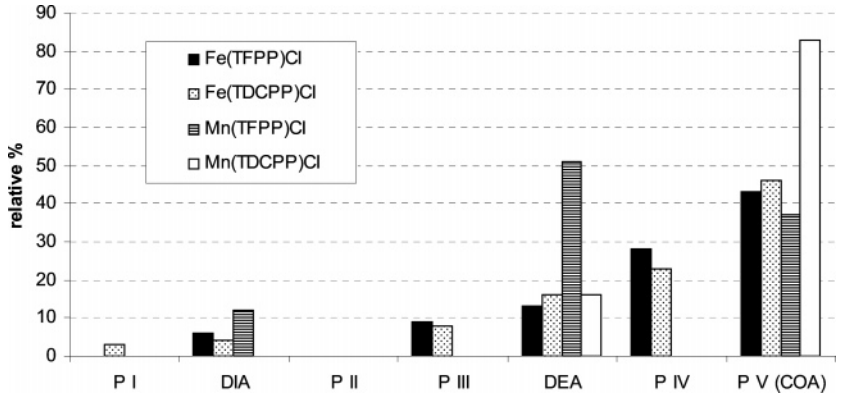

Figure 5. Product distribution (in percentage) obtained in the metalloporphyrin-catalyzed oxidation of ATZ by *m*-CPBA in ACN in the standard conditions. P I, P II, P III, P IV, and P V are unknown products.

Table 2. Total Yield of the Metalloporphyrin-Catalyzed ATZ Oxidation Reactions, under Different Reaction Conditions

catalyst	oxidant		MeOH (*R*%)	ACN (*R*%)
Fe(TFPP)Cl	1	PhIO	~1	10
	2	*m*-CPBA	2	10
Fe(TDCPP)Cl	3	PhIO	~1	8
	4	*m*-CPBA	~1	14
Mn(TFPP)Cl	5	PhIO	~1	32
	6	*m*-CPBA	~1	11
Mn(TDCPP)Cl	7	PhIO	~1	3
	8	*m*-CPBA	~1	10

activity remained low even upon changes in the porphyrin ligand ($TFPP^{2-}$ and $TDCPP^{2-}$; **Figure 2**), metal (Fe^{3+} and Mn^{3+}), and oxidant (PhIO and *m*-CPBA). Therefore, these three variables are not the main variables responsible for the low yields. A possible explanation for the inefficiency of these systems could be the fact that the solvent MeOH could be acting as substrate, thus competing with ATZ for the catalytic species. To investigate whether this was the case, formaldehyde, the oxidation product generated from MeOH, was quantified by means of the Nash test (*21*, *22*) in the case of the Fe(TFPP)Cl/PhIO and Mn(TFPP)Cl/PhIO systems. The Nash test consists of the spectrophotometric determination of formaldehyde, which, in the presence of a diketone and an ammonium salt, forms diacetylhydrolutidine (DDL), a compound that absorbs at 412 nm.

By means of a calibration curve previously built from standard solutions, the concentration of the formaldehyde generated in the reaction could be calculated, and the percentage of oxidized methanol could thus be estimated. Both in the presence and in the absence of ATZ, the yield of formaldehyde was 75% in the case of both Fe(TFPP)Cl and Mn(TFPP)Cl. This result shows that the low yields obtained in the ATZ oxidation reactions carried out in MeOH are because this solvent is preferentially oxidized in these conditions, thus consuming 75% of the oxidant present in the reaction medium.

In ACN, a solvent that does not compete with ATZ for the catalytically active species, the metalloporphyrins were able to oxidize the herbicide with total oxidation product yields as high as 32%, in the case of the Mn(TFPP)Cl/PhIO system (**Table 2**, entry 5). This result demonstrates that these metalloporphyrin complexes are good catalysts, especially if we consider that ATZ is a herbicide that persists in the environment and that its degradation is difficult even in the presence of advanced oxidation processes (*13*, *14*).

By analyzing the product distribution obtained in the metalloporphyrin-catalyzed oxidation of ATZ in ACN (**Figures 4** and **5**), it can be seen that the metabolite DEA was one of the main products in all the reactions. In some reactions, formation of the metabolite DIA was also detected. These two compounds correspond to the main metabolites obtained in the ATZ metabolism by cytochrome P450 in vivo (*10*−*12*), which indicates that the metalloporphyrins used here can be considered biomimetic models of this enzyme.

Apart from the metabolites DEA and DIA, we also detected the formation of five other products during ATZ oxidation, which were designated P I, P II, P III, P IV, and P V, according to the elution order. Compound P V was the most abundant product for all the metalloporphyrin/oxidant systems, except for Mn(TFPP)Cl/*m*-CPBA, which led to DEA as the main product (**Figure 5**). Compound P V was isolated and analyzed by mass spectrometry (ESI/MS) and ESI-MS/MS in the positive mode. This compound gave rise to a signal at *m*/*z* 230, which

Table 3. Main Fragments of the Products DEA and P V Generated during the Oxidation of ATZ as Determined by ESI-MS and ESI-MS/MS

compound	$[M + H^+]$	ESI-MS/MS (*m*/*z*)
DEA	188	188, 146, 110, 104, 79, 68
PDV	230	230, 188, 146, 110, 104, 79, 68

corresponds to the molecular ion $[M + H^+]$, and a fragmentation MS/MS pattern similar to DEA, as shown in **Table 3**. Comparison of these results with literature data for compounds generated from atrazine degradation (*13*, *14*) leads to the identification of P V as a compound containing an amide in the ethyl chain of ATZ (COA; **Figure 6**). Studies reporting ATZ

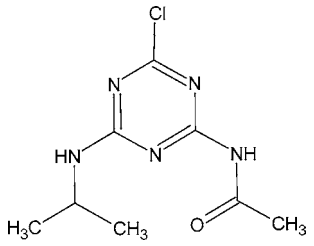

Figure 6. Structure of COA, as determined by MS and MS/MS spectrometry.

degradation via advanced oxidation processes have described COA as an intermediate compound in the formation of the metabolite DEA (*13*, *14*, *23*, *24*).

Identification of the remaining unknown products (P II−IV) was not possible because they were formed at very low concentrations, even though P IV was the second most abundant product in the case of the ironporphyrin/*m*-CPBA systems. P IV is probably formed via a radicalar mechanism, once its formation coincides with the use of the peracid as oxidant, which may undergo homolytic cleavage and generate radicals.

Although the P450 system is capable of N-dealkylating two alkyl side chains of the herbicide in vivo, which leads to the formation of the metabolites DEA, DIA, and DAA, the metalloporphyrin systems preferentially attach the ethyl chain in ATZ, generating the compound COA and the metabolite DEA as the main products, as well as traces of the metabolite DIA. This preference was confirmed when the metabolites DEA and DIA were used as substrates for the Fe(TFPP)Cl/PhIO/ACN system in the standard conditions established in this work. When the metabolite DIA was used as substrate, formation of the metabolite DAA was detected in 10% yield, as expected. However, when the metabolite DEA was employed as substrate, there was no formation of DAA. In other words, attack of the catalytically active species to the propyl chain is not favored, and only traces of the compound OHDEA (yield ∼1%) were obtained. The propyl chain probably confers higher steric hindrance to the approach of the high-valent oxo-metal species generated from the metalloporphyrins used in this study, which all contain bulky substituents (−Cl and −F) in the phenyl substituents on the porphyrin ring.

The different results obtained with the metalloporphyrin models when compared with those obtained with the enzyme demonstrate the importance of the protein matrix involving the iron porphyrin in P450. The matrix is responsible for directing the substrate approach, through the interaction with specific amino acids, thus controlling the oxidation site. Biomimetic models cannot reproduce such control.

As an attempt to understand the mechanism of metalloporphyrin-catalyzed ATZ oxidation and the formation of the various products, some variables such as reaction time, excess oxidant,

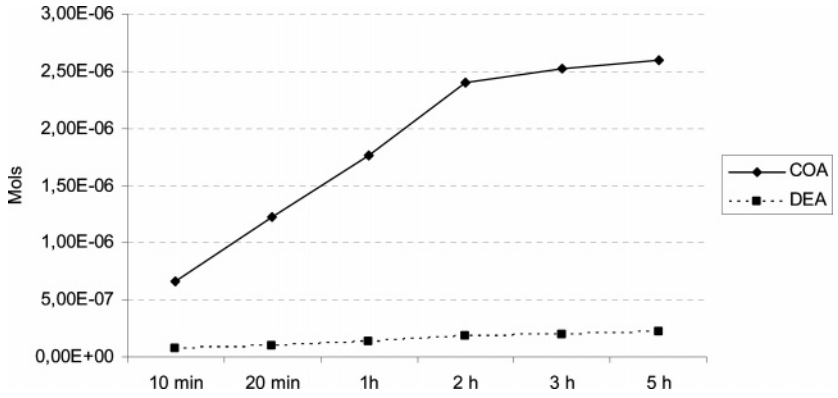

Figure 7. Number of mol of COA and DEA as a function of time obtained in AZT oxidation by the Fe(TFPP)Cl/PhIO/ACN system.

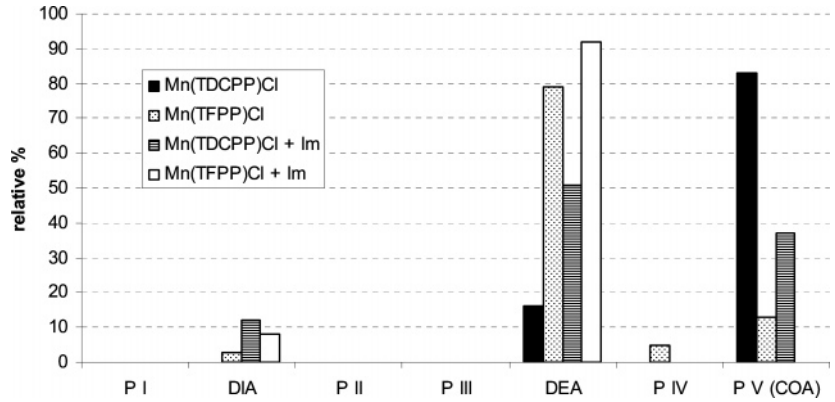

Figure 8. Product distribution obtained in the MnP-catalyzed ATZ oxidation by m-CPBA in ACN, in the standard conditions and in the presence of imidazole. P I, P II, P III, P IV, and P V are unknown products.

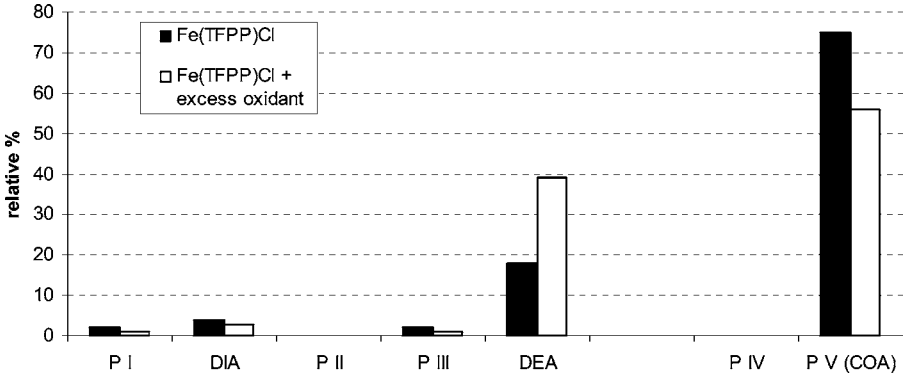

Figure 9. Product distribution in percentage, obtained in the Fe(TFPP)Cl-catalyzed ATZ oxidation by PhIO in ACN, in the standard conditions and in excess oxidant. P I, P II, P III, P IV, and P V are unknown products.

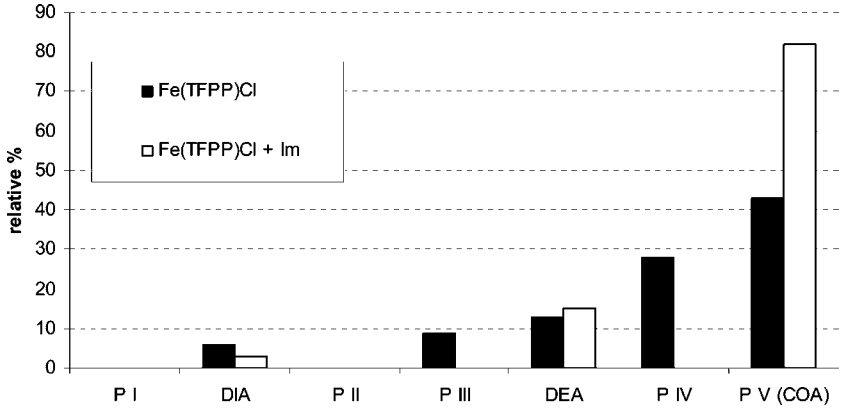

Figure 10. Product distribution, in percentage, obtained in the FeP-catalyzed AZT oxidation by *m*-CPBA in ACN in the standard conditions and in the presence of imidazole. P I, P II, P III, P IV, and P V are unknown products.

presence of imidazole, and absence of O_2 (argon atmosphere) were evaluated.

Because the compound COA is an intermediate in the formation of the metabolite DEA in ATZ degradation studies using advanced oxidation mechanisms (*13*, *14*, *23*, *24*), the reaction using the Fe(TFPP)Cl/PhIO/ACN system under the standard conditions was monitored as a function of time (10 min, 20 min, 1 h, 2 h, 3 h, and 5 h). This was done to investigate whether formation of the metabolite DEA occurred via COA consumption. **Figure 7** shows a plot of the number of mol of each of the main reaction products (COA and DEA) versus the reaction time. It was observed that the compound COA and the metabolite DEA are formed independently, contrary to what is reported in the literature for other catalytic systems (*13*, *14*, *23*, *24*).

Results obtained in the reactions carried out in the presence of imidazole also confirm our findings. The effect of imidazole was evaluated for the metalloporphyrins Mn(TFPP)Cl, Mn(TDCPP)Cl, and Fe(TFPP)Cl, using *m*-CPBA as oxidant. Nitrogen ligands, such as imidazole, act as cocatalysts in systems involving manganese porphyrins, leading to increased reaction rates, catalytic yields, and selectivity (*25*, *26*). This is because these ligands can coordinate to the manganese porphyrin in the position trans to the metal-oxo bond, thus stabilizing the intermediate catalytic species $Mn^{V}OP$. This intermediate is responsible for efficient stereoselective oxidations. The presence of imidazole also prevents reduction of the $Mn^{V}OP$ species to $Mn^{IV}OP$, which is responsible for nonselective and little efficient radicalar reactions (*25*, *26*). Imidazole also acts as an acid−base catalyst, favoring heterolytic cleavage of the peroxide bond, with formation of the high-valent oxo-metal intermediate, thus preventing radical formation (*26*).

Figure 8 shows the product distribution for the MnP/*m*-CPBA systems in both the presence and absence of imidazole. It can be seen that imidazole favors formation of the metabolite DEA, with concomitant decrease in the formation of the compound COA, or even its absence. This result shows that these two products are formed via distinct and competitive mechanisms, which involve different catalytically active species. The metabolite DEA is probably formed via the $Mn^{V}OP$ species, which is stabilized by imidazole (*25*), whereas COA is formed via the $Mn^{IV}OP$ intermediate, which can be formed by reduction of $Mn^{V}OP$ in the absence of the nitrogen ligand (*25*).

Analogously, in the case of iron porphyrins, the metabolite DEA would be formed via the catalytic species $Fe^{IV}OP^{\bullet+}$ (or $Fe^{V}OP$), mimicking the P450 metabolism in vivo, whereas COA would be formed via the $Fe^{IV}OP$ species.

Involvement of the $Fe^{IV}OP$ species in these reactions in the absence of the imidazole was confirmed by the bright orange color acquired by the reaction solution after the addition of the oxidant, which is typical of this species (*27*). Preliminary studies of the reaction intermediates by UV−vis and EPR at low temperature also confirmed the presence of this species, which is characterized by absorption bands at 545 and 410 nm (Soret band) in the UV−vis spectrum (*20*, *28*). This species also led to the disappearance of the high-spin Fe(III) signal ($S = 5/2$, $g = 6.0$) in the EPR spectrum because of the formation of an EPR silent Fe^{IV} species (*29*).

An increase in the yield of metabolite DEA, with concomitant decrease in the formation of compound COA, could also be seen in reactions carried out with excess oxidant in the case of the Fe(TFPP)Cl/ACN/PhIO system (catalyst/oxidant/substrate molar ratio of 1:240:120; **Figure 9**). In these conditions, it is probable that COA undergoes further oxidation as a result of

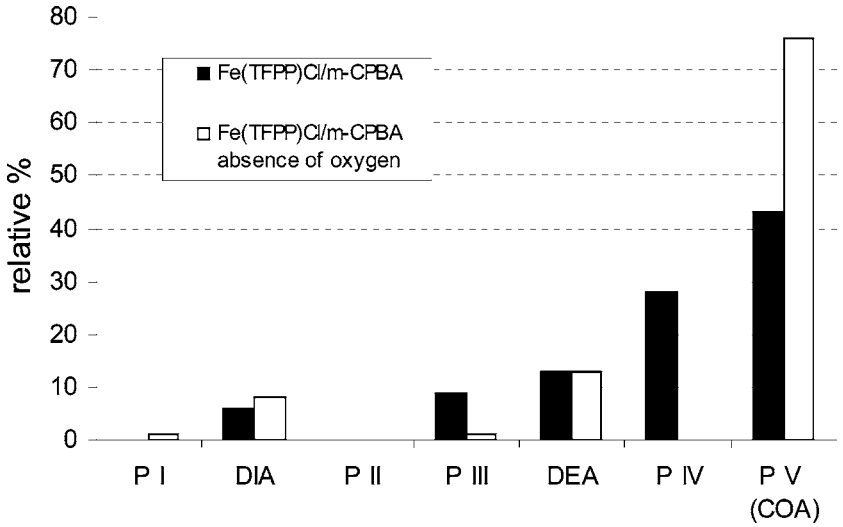

Figure 11. Product distribution, in percentage, obtained in the FeP-catalyzed AZT oxidation by *m*-CPBA in ACN in the standard conditions and in the absence of oxygen. P I, P II, P III, P IV, and P V are unknown products.

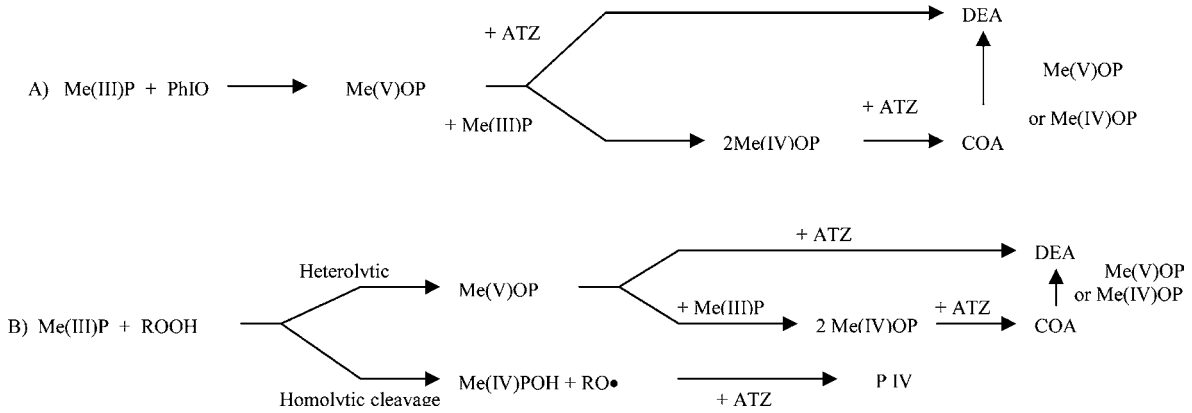

Figure 12. Scheme for MeP-catalyzed AZT oxidation.

the excess oxidant. This should lead to the formation of DEA, as shown by the increase in the concentration of this product in **Figure 9**.

No significant alterations in the DEA/COA ratio were observed for the Fe(TFPP)Cl/*m*-CPBA/ACN system in the presence of imidazole (**Figure 10**). Contrary to manganese porphyrins, the cocatalytic effect of the nitrogen ligand is not expected in this case. This is because imidazole bis-coordinates to the axial positions of the iron porphyrin, thus blocking the catalytic site and the formation of the catalytic species (*30*). Therefore, imidazole was used in this case aiming at favoring heterolytic cleavage of the peracid O−O bond via acid catalysis, which should lead to formation of the oxo-ferryl porphyrin π-cation radical, as well as hinder formation of RO$^{\bullet}$ radicals via peroxide homolytic cleavage. **Figure 10** shows that the presence of imidazole avoids formation of P IV and increases production of COA. Bearing in mind that P IV is produced only in reactions employing the peracid as oxidant, the absence of this product in a system using *m*-CPBA in the presence of imidazole confirms that P IV really results from the homolytic cleavage of the peracid O−O bond.

The absence of P IV and an increase in COA concentration are also observed when the reaction using the Fe(TFPP)Cl/*m*-CPBA/ACN system is carried out under argon atmosphere (**Figure 11**). This also confirms that P IV is formed via the radicalar mechanism propagated by O_2 present in the reaction medium.

Taking the product distribution under the different conditions studied here and the above-discussed hypotheses into account, it is possible to propose a scheme for metalloporphyrin-catalyzed ATZ oxidation as shown in **Figure 12**.

Scheme A in **Figure 12** considers the use of PhIO as oxidant. After formation of the active species, Me^{V}OP in this case, the reaction may follow two pathways. The first one is biomimetic and involves reaction of the active species with ATZ, leading to the formation of the metabolite DEA. The second pathway corresponds to the reaction between the active species and another catalyst molecule, leading to formation of the species Me^{IV}OP. The latter reacts with ATZ, producing COA. Once ATZ is a relatively inert substrate, the second pathway is favored, so the main reaction product is COA. Because COA is an intermediate species to DEA, it is possible that it is oxidized again to DEA under certain conditions, such as in the presence of excess oxidant.

Scheme B in **Figure 12** considers the use of the peracid as oxidant. Formation of the species Me^{V}OP depends on the heterolytic cleavage of the metal-oxo bond, which is favored in the presence of imidazole. Formation of this species takes us to the first pathway in scheme A, which was discussed above. Homolytic cleavage of the metal-oxo bond leads to the formation of the species Me^{IV}POH and of radicals represented by RO$^{\bullet}$, as well as of other radicals associated with molecular oxygen, present in the reaction medium. These should lead to P IV and other byproducts of radicalar reactions.

In conclusion, this work has demonstrated the ability of metalloporphyrins to mimic the action of P450 in the oxidation of atrazine, a highly persistent herbicide, as well as their capacity to mimic the in vivo action of P450, with formation of two of the metabolites found in plants: DEA and DIA.

Our studies also showed the potential application of these biomimetic chemical models in studies that pursue the elucidation of the in vivo metabolism of herbicides, thus overcoming the difficulty in working with enzymes in vitro.

As in the case of studies on drug oxidation, it can be envisaged that metalloporphyrins will become an important tool for the understanding of herbicide metabolism, and they will help elucidate some resistance mechanisms developed by weeds, thus assisting the development of novel compounds for pest control in agriculture.

ACKNOWLEDGMENT

We thank Dr. Akira Ueda, from Syngenta, for kindly supplying atrazine. We also thank Professor Otaciro R. Nascimento for the EPR analysis.

LITERATURE CITED

(1) Reichhart, D. W.; Hehn, A.; Didieriean, L. Cytochrome P450 for engineering herbicide tolerance. *Trends Plant Sci.* **2000**, *5*, 116−123.

(2) Coleman, J.; Blake-Kalff, M.; Davies, E. Detoxification of xenobiotics by plants: chemical modification and vacuolar compartmentation. *Trends Plant Sci.* **1997**, *2*, 144−151.

(3) Fragoso, D. B.; Guedes, R. N. C.; Ladeira, J. A. Selection in the evolution of resistance to organophosphates in *Leucoptera coffeella*. *Neotrop. Entomol*. **2003**, *32*, 329−334.

(4) Bernadou, J.; Meunier, B. Biomimetic Chemical Catalysts in the Oxidative Activation of Drugs. *Adv. Synth. Catal.* **2004**, *346*, 171−184.

(5) Meunier, B.; Robert, A.; Pratviel, G. Metalloporphyrins in catalytic oxidations and oxidative DNA cleavage. In *The Porphyrin Handbook*; Kadish, K. M., Smith, K. M., Guilard, R., Eds.; Academic Press: New York, **2000**; pp 119−187.

(6) Santos, A. C. M. A.; Smith, J. R. L.; Assis, M. D. Chloroquine-iron(III) tetra-arylporphyrin interactions and their effect on chloroquine oxidations catalyzed by iron(III) tetra-arylporphyrin. *J. Porphyrins Phthalocyanines* **2005**, *9*, 326−333.

(7) Keserü, G. M.; Balogh, G.; Czudor, I.; Karancsi, T.; Fehér, A.; Bertók, B. Chemical Models of Cytochrome P450 Catalyzed Insecticide Metabolism. Application to the Oxidative Metabolism of Carbamate Insecticides. *J. Agric. Food Chem.* **1999**, *47*, 762−769.

(8) Fukushima, M.; Fujisawa, T.; Katagi, T. Tomato Metabolism and Porphyrin-Catalyzed Oxidation of Pyriproxyfen. *J. Agric. Food Chem*. **2005**, *53*, 5353−5358.

(9) Topal, A.; Adams, N.; Hodgson, E.; Kelly, S. L. In vitro metabolism of atrazine by tulip cytochrome P450. *Chemosphere* **1996**, *32*, 1445−1451.

(10) Hanioka, N.; Jinno, H.; Kitazawa, K.; Tanaka-Kagawa, T.; Nishimura, T.; Ando, M.; Ogawa, K. In vitro biotransformation of atrazine by rat liver microsomal cytochrome P450 enzymes. *Chem.-Biol. Interact.* **1998**, *116*, 181−198.

(11) Cherifi, M.; Raveton, M.; Picciocchi, A.; Ravanel, P.; Tissut, M. Atrazine metabolism in corn seedlings. *Plant Physiol. Biochem.* **2001**, *39*, 665−672.

(12) Ohkawa, H.; Tsujii, H.; Ohkawa, Y. The use of cytochrome P450 genes to introduce herbicide tolerance in crops: a review. *Pestic. Sci.* **1999**, *55*, 867−874.

(13) Arnold, S. M.; Hickey, W. J.; Harris, R. F. Degradation of Atrazine by Fenton's Reagent: Condition Optimization and Product Quantification. *Environ. Sci. Technol.* **1995**, *29*, 2083−2089.

(14) Chan, K. H.; Chu, W. Atrazine removal by catalytic oxidation processes with or without UV irradiation: Part II: an analysis of the reaction mechanisms using LC/ESI-tandem mass spectrometry. *Appl. Catal., B* **2005**, *58*, 165−174.

(15) Sharefkin, J. G.; Saltzman, H. Iodosobenzene. *Organic Syntheses*; Wiley & Sons: New York, 1973; Collect. Vol. 5, p 658.

(16) Adler, A. D.; Longo, F. R.; Kampas, F.; Kim, J. On the preparation of metalloporphyrins. *J. Inorg. Nucl. Chem.* **1970**, *32*, 2443−2445.

(17) Nash, T. Colorimetric determination of formaldehyde under mild conditions. *Nature* **1952**, *170*, 976.

(18) Karki, S. B.; Dinnocenzo, J. P.; Jones, J. P.; Korzekwa, K. R. Mechanism of Oxidative Amine Dealkylation of Substituted *N*,*N*-Dimethylanilines by Cytochrome P-450: Application of Isotope Effect Profiles. *J. Am. Chem. Soc.* **1995**, *117*, 3657−3664.

(19) Groves, J. T. High-valent iron in chemical and biological oxidations *J. Inorg. Biochem*. **2006**, *100*, 434−447.

(20) Nam, W.; Han, H. J.; Oh, S. Y.; Lee, Y. J.; Choi, M. H.; Han, S. Y.; Kim, C.; Woo, S. K.; Shin, W. New Insights into the Mechanisms of O−O Bond Cleavage of Hydrogen Peroxide and *tert*-Alkyl Hydroperoxides by Iron(III) Porphyrin Complexes. *J. Am. Chem. Soc.* **2000**, *122*, 8677−8684.

(21) Guedes, A. A.; Santos, A. C. M.; Assis, M. D. Some factors influencing the selectivity of styrene oxidation by active oxygen donors catalyzed by three generations of ironporphyrins. *Kinet. Catal.* **2006**, *47*, 572−580.

(22) Schiavon, M. A.; Iamamoto, Y.; Nascimento, O. R.; Assis, M. D. Catalytic activity of nitro- and carboxy-substituted iron porphyrins in hydrocarbon oxidation: Homogeneous solution and supported systems. *J. Mol. Catal. A: Chem.* **2001**, *174*, 213−222.

(23) Kawahigashi, H.; Hirose, S.; Ohkawa, H.; Ohkawa, Y. Phytoremediation of the herbicides atrazine and metolachlor by transgenic rice plants expressing human CYP1A1, CYP2B6, and CYP2C19. *J. Agric. Food Chem.* **2006**, *54*, 2985−2991.

(24) Ross, M. K.; Filipov, N. M. Determination of atrazine and its metabolites in mouse urine and plasma by LC−MS analysis. *Anal. Biochem.* **2006**, *351*, 161−173.

(25) Gunter, M. J.; Turner, P. The role of the axial ligand in mesotetraarylmetalloporphyrin models of the P-450 cytochromes. *J. Mol. Catal.* **1991**, *66*, 121−126.

(26) Battioni, P.; Renaud, J. P.; Bartoli, J. F.; Artiles, M. R.; Fort, M.; Mansuy, D. Monooxygenase-like Oxidation of Hydrocarbons by Hydrogen Peroxide Catalyzed by Manganese Porphyrins and Imidazole: Selection of the Best Catalytic System and Nature of the Active Oxygen Species. *J. Am. Chem. Soc*. **1988**, *110*, 8462−8463.

(27) Bell, S. E. J.; Cooke, P. R.; Inchley, P.; Leanord, D. R.; Smith, J. R. L. Oxoiron(IV) porphyrins derived from charged iron(III) tetraarylporphyrins and chemical oxidants in aqueous and methanolic solutions. *J. Chem. Soc., Perkin Trans*. **1991**, *2*, 549−559.

(28) Fujii, H. Eletronic structure and reactivity of high-valent oxo iron porphyrin. *Coord. Chem. Rev.* **2002**, *226*, 51−60.

(29) Assis, M. D.; Serra, O. A.; Iamamoto, Y.; Nascimento, O. R. An EPR and electronic spectroscopy study of intermediates in a mono *o*-nitro substituted iron porphyrin reaction with iodosylbenzene. *Inorg. Chim. Acta* **1991**, *187*, 107−114.

(30) Evans, S.; Lindsay-Smith, J. R. The oxidation of ethylbenzene and other alkylaromatics by dioxygen catalysed by iron(III) tetrakis(pentafluorophenyl)porphyrin and related iron porphyrins. *J. Chem. Soc., Perkin Trans. 2* **2000**, 1541−1551.

Received for review August 28, 2006. Revised manuscript received October 24, 2006. Accepted October 24, 2006. We thank the Brazilian agencies FAPESP, CNPq, and CAPES for financial support.

JF062462N